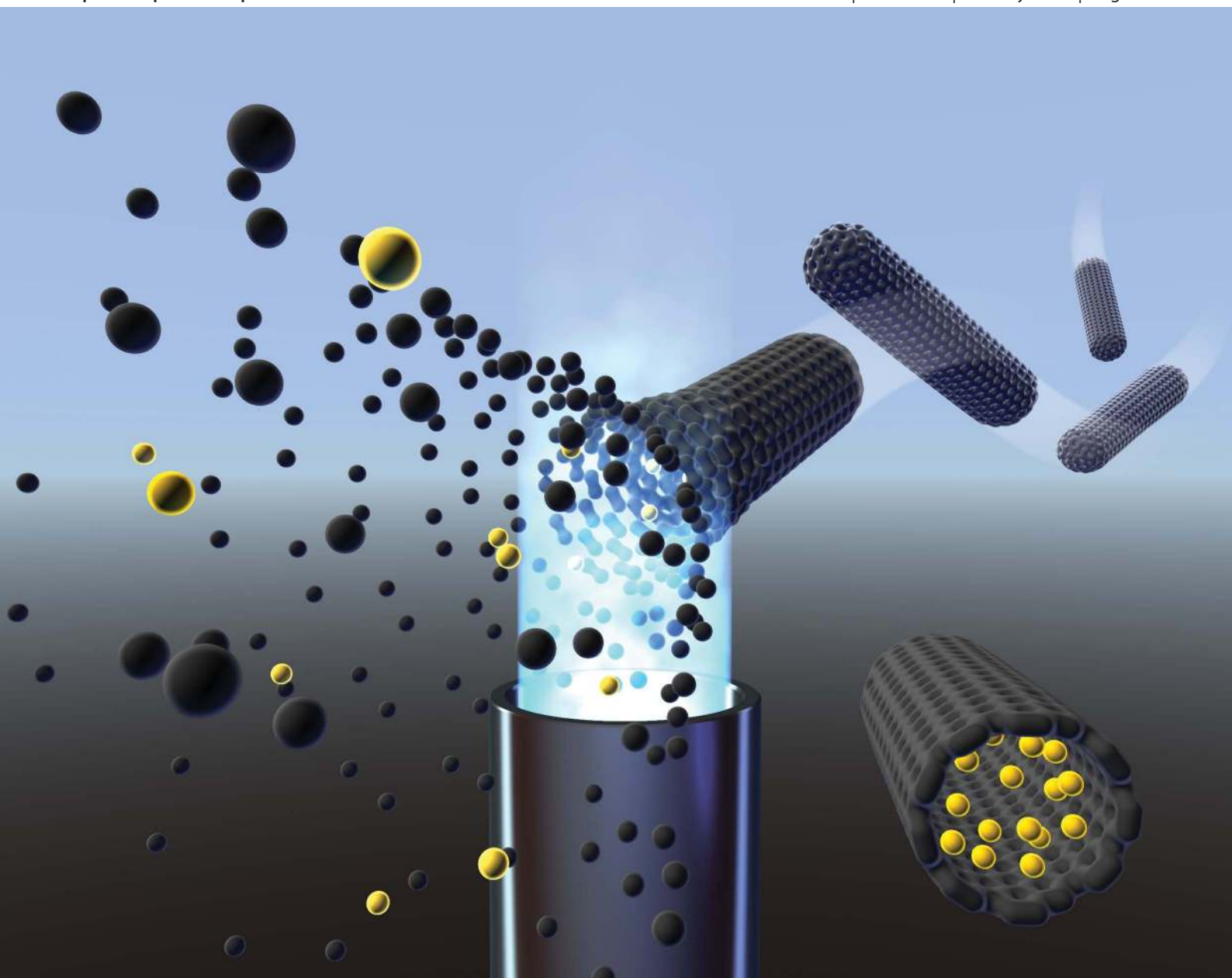


# Environmental Science Processes & Impacts

Formerly Journal of Environmental Monitoring

<http://rsc.li/process-impacts>

Volume 15 | Number 1 | January 2013 | Pages 1–316



Themed issue: Anthropogenic nanoparticles in the environment

ISSN 2050-7887

RSC Publishing

PAPER

James F. Ranville *et al.*

Detection of single walled carbon nanotubes by monitoring embedded metals



2050-7887 (2013) 15:1;1-#

## Detection of single walled carbon nanotubes by monitoring embedded metals†

Cite this: *Environ. Sci.: Processes Impacts*, 2013, **15**, 204

Robert B. Reed,<sup>a</sup> David G. Goodwin,<sup>b</sup> Kristofer L. Marsh,<sup>b</sup> Sonja S. Capracotta,<sup>c</sup> Christopher P. Higgins,<sup>d</sup> D. Howard Fairbrother<sup>b</sup> and James F. Ranville<sup>\*a</sup>

Detection of single walled carbon nanotubes (CNTs) was performed using single particle-inductively coupled plasma-mass spectrometry (spICPMS). Due to the ambiguities inherent in detecting CNTs by carbon analysis, particularly in complex environmental matrices, this study focuses on using trace catalytic metals intercalated in the CNT structure as proxies for the nanotubes. Using a suite of commercially available CNTs, the monoisotopic elements Co and Y were found to be the most effective for differentiation of particulate pulses from background. The small, variable, amount of trace metal in each CNT makes separation from instrumental background challenging; multiple cut-offs for determining CNT number concentration were investigated to maximize the number of CNTs detected and minimize the number of false positives in the blanks. In simple solutions the number of CNT pulses detected increased linearly with concentration in the  $\text{ng L}^{-1}$  range. However, analysis of split samples by both spICPMS and Nanoparticle Tracking Analysis (NTA) showed the quantification of particle number concentration by spICPMS to be several orders of magnitude lower than by NTA. We postulate that this is a consequence of metal content and/or size, caused by the presence of many CNTs that do not contain enough metal to be above the instrument detection limit, resulting in undercounting CNTs by spICPMS. However, since the detection of CNTs at low  $\text{ng L}^{-1}$  concentrations is not possible by other techniques, spICPMS is still a more sensitive technique for detecting the presence of CNTs in environmental, materials, or biological applications. To highlight the potential of spICPMS in environmental studies the release of CNTs from polymer nanocomposites into solution was monitored, showcasing the technique's ability to detect changes in released CNT concentrations as a function of CNT loading.

Received 26th August 2012  
Accepted 6th November 2012

DOI: 10.1039/c2em30717k

rsc.li/process-impacts

### Environmental impact

As predicted environmental concentrations of carbon nanotubes (CNTs) are in the  $\text{ng L}^{-1}$  range, extremely sensitive analytical techniques are required for detection of these materials. The research presented in this manuscript examines the use of single particle inductively coupled plasma mass spectrometry (spICPMS) for detection of CNTs by monitoring metal nanoparticle catalysts embedded in the carbon structure as a proxy for the CNTs themselves. This work addresses the challenge associated with differentiating metal proxy signal from background, which is a challenge applicable to analysis of many polydisperse nanomaterials, such as CNTs, by spICPMS. Release of CNTs from a CNT–chitosan nanocomposite showed the ability of spICPMS to qualitatively detect increases in CNT concentration with increased loading in the polymer matrix.

### Introduction

Increased production and use of engineered nanomaterials (NMs) over the last 5 years<sup>1</sup> and growing concern about the

potential hazards of these materials has prompted a need for improvements in detection and characterization methods. Carbon-based NMs, such as fullerenes and carbon nanotubes (CNTs), are contained in more consumer products than any other NM except for silver.<sup>1</sup> Specifically, concern regarding exposure to CNTs in the manufacturing process, and their potential release into the environment from CNT-containing composites, drives the need for analytical techniques capable of detecting these materials. Mechanical agitation of CNTs during manufacturing has been shown to result in detectable concentrations of airborne particulates.<sup>2</sup> In this case, CNTs may cause dermal toxicity,<sup>3</sup> but more importantly they have the potential for pulmonary toxicity due to their morphological similarity to

<sup>a</sup>Department of Chemistry and Geochemistry, Colorado School of Mines, Golden, CO 80401, USA. E-mail: jranvill@mines.edu

<sup>b</sup>Department of Chemistry, Johns Hopkins University, Baltimore, MD, 21218, USA

<sup>c</sup>School of Public Health I, Ann Arbor, MI, 48109, USA

<sup>d</sup>Department of Civil and Environmental Engineering, Colorado School of Mines, Golden, CO 80401, USA

† Electronic supplementary information (ESI) available. See DOI: 10.1039/c2em30717k

asbestos.<sup>4,5</sup> Airborne concentrations in the immediate vicinity of manufacturing processes may far exceed those predicted in the environment ( $\mu\text{g m}^{-3}$  vs.  $\text{pg m}^{-3}$  respectively<sup>2,6</sup>), but there is still potential ecotoxicological risk associated with CNTs. Incorporation of CNTs into a variety of consumer products creates the potential for release of these materials to the environment with subsequent transport and transformation processes.<sup>7</sup> Expected aqueous environmental concentrations of CNTs ( $\sim\text{ng L}^{-1}$ )<sup>6,8</sup> are currently well below concentrations used in laboratory toxicity tests, which are often in the  $\text{mg L}^{-1}$  range.<sup>9–11</sup> This “concentration gap” for particle detection provides strong motivation for development of metrology capable of detecting extremely small amounts of NMs.

Methods to detect environmentally relevant concentrations of CNTs are rare. Those commonly used for characterization of CNTs, such as transmission electron microscopy, scanning tunnelling microscopy, UV-Vis and Raman spectroscopy,<sup>12</sup> do not have the capability to efficiently detect the low concentrations expected in the environment, although near infrared fluorescence spectroscopy has been used to analyze CNTs in sediments and tissues.<sup>13</sup> In contrast, inductively coupled plasma-mass spectrometry (ICP-MS) has detection limits at the  $\text{ng L}^{-1}$  or sub- $\text{ng L}^{-1}$  level for most elements. However, carbon is generally not detectable with standard ICP-MS methods although synthesis of CNTs typically utilizes metals such as Mo, Ni, Co, Y, and Fe<sup>14,15</sup> for catalytic growth of the carbon structure. Consequently, residual metal catalyst particles frequently persist in the CNT structure after manufacture<sup>16</sup> and have been associated with toxicity to organisms *via* generation of reactive oxygen species.<sup>3</sup> CNTs are often purified after synthesis to remove metal impurities,<sup>17</sup> but even after acid purification metals intercalated within carbon structures typically account for several percent of the particle mass.<sup>18,19</sup> Quantification of metal impurities in CNTs has been performed by ICP-MS<sup>20,21</sup> for analysis of bulk metal content; however, we are interested in the ability to use these metals as a route to detect and quantify CNTs at the extremely low concentrations likely to be encountered in the environment.

Specifically, the goal of this study was to evaluate the ability of single particle ICP-MS (spICPMS) to detect trace catalytic metals intercalated in CNTs as proxies for the materials themselves. Initially developed for metal colloid analysis by Deguelle and Favarger,<sup>22</sup> spICPMS has recently been used for detection, quantitation of particle number, and sizing of engineered nanoparticles such as Ag<sup>23–25</sup> and metal oxides such as TiO<sub>2</sub> and CeO<sub>2</sub>.<sup>26</sup> An in-depth discussion of the theory behind this technique can be found in these previous studies. In brief, NMs entering the plasma are disintegrated to a packet of ions. Consequently, metals appear as individual pulses that are distinguished from the background, with the ion intensity being directly related to the number of analyte atoms in the NM. The instrument signal is reported as counts of the analyte isotope per dwell time or reading, *e.g.* <sup>89</sup>Y counts per 10 ms. Size information on chemically uniform, (roughly) spherical NMs, such as metals or metal oxides, can be extracted from spICPMS.<sup>23,25</sup> For rod-like NMs length distributions can be determined if the minor dimensions have been determined

from SEM/TEM data.<sup>26</sup> One of the challenges inherent in using spICPMS for CNT analysis is that variable metal contents among individual CNTs makes size/length estimation impossible unless the bulk metal content is applied to all CNTs, although sizing was not the focus of this study.

In contrast to sizing, a determination of particle number concentrations from spICPMS is more direct and relies on applying the transport efficiency to the observed pulse frequency. As in previous publications,<sup>25,27</sup> we define transport efficiency as the fraction of sample droplets, containing NM and/or dissolved analytes, which reach the plasma. Determination of number concentration is, however, strongly affected by what criterion is used for defining a pulse as opposed to background noise. This is especially true for polydisperse samples having a significant population of small particles that cannot be separated from the background. This will be an issue for single walled CNTs due to heterogeneity in both the size and number of metals that are embedded within the carbon cylinder.

Another important consideration in the design and implementation of appropriate analytical techniques for NM detection is the issue of selectivity. Aqueous environmental matrices are extremely heterogeneous, and NM concentrations are expected to be many orders of magnitude lower than that of other particles and soluble chemicals present. This issue is particularly important for CNTs due to the prevalence of naturally occurring carbon-containing species (*i.e.* cells, organic detritus, humics). This is exacerbated in the case of biological tissues where detection of CNTs by carbon analysis is clearly not possible. Therefore, using metals as a surrogate to detect the presence of CNTs with spICPMS could provide a superior means of differentiation of CNTs from other materials even when CNTs are present at extremely low concentrations.

The first goal of this study was to assess the ability of spICPMS to detect CNTs using trace metal catalysts as proxies. Further investigation of this method's capabilities for detection and quantification of CNTs at environmentally relevant concentrations was carried out: the end goal of this work was to determine if spICPMS could be used to detect and quantify CNTs in a simulated release study. To the best of our knowledge, this is the first work to use spICPMS as a detection method for CNTs in any application.

## Materials and methods

### Preparation of CNT suspensions

The CNTs used for this study were acquired from Nanostructured and Amorphous Material (NanoAmor) (1280 NMG), Carbon Solutions (AP-SWNT), and Southwest NanoTechnologies (SG65). The CNTs used were not surface modified. Stock CNT solutions were prepared by initially adding a known CNT mass to a known volume of DI water that contained 1% w/w Triton™-X-100 (Sigma-Aldrich). The CNTs were suspended by sonicating the mixture overnight in a low power (70 W) Branson 1510 ultrasonicator. At this stage the stock solutions were sent from JHU to CSM for ICP-MS analysis. Prior to ICP-MS analysis all stock CNT solutions were diluted to concentrations in the

ng L<sup>-1</sup> range using 18 Ω nanopure water (Barnstead Nanopure) in 15 mL polypropylene centrifuge tubes. Suspensions were homogenized after each dilution by immersion in a bath sonicator (Fisher, FS60H, 150 W) for 10 minutes. Optimal concentrations varied among the samples and were chosen to avoid coincidence while providing sufficient counts for statistical robustness.<sup>26</sup> DI blanks were analyzed for each metal isotope used for CNT detection, and each sample was run in duplicate to evaluate reproducibility. To determine the amount of soluble metal released from the CNTs, a separate set of CNT suspensions were prepared in nanopure water, which were then centrifuged for 1 hour at 125 000 g (Optima XL, Beckman) to remove the CNTs. This supernatant was used to compare to deionized water in determining the level of background counts. Dissolved Au, Co, and Y calibration standards were prepared using Claritas PPT (SPEX Certiprep) ICP-MS standard grade stock solutions. A gold nanoparticle standard (100 nm) was used for quantification of instrument efficiency and was purchased from British Biocell International (BBI).

### Characterization of CNTs

Bulk physical and chemical characterization involved Energy Dispersive Spectroscopy (EDS) analysis, which was performed using a cold cathode field emission scanning electron microscope (SEM; JEOL 6700F) equipped with an EDAX Genesis 4000 X-ray analysis system (detector resolution of 129 eV).

### Comparison of spICPMS and NTA

A Perkin Elmer NexION 300q with an S10 autosampler, using 20 000 dwell times (10 ms dwell time, total data collection time = 200 seconds per sample), provided the spICPMS data for both CNT suspensions and dissolved standards and blanks. The sample introduction rate in all experiments was 0.97 mL min<sup>-1</sup>. Given the ability of spICPMS to detect the presence of a very small number of metal nanoparticles, extra caution was needed to avoid sample carry over. Methods included rinsing of the nebulizer and spray chamber, as well as daily changes of the peristaltic pump tubing, which also minimized flow rate drift.

To compare particle number measurements from spICPMS and Nano Tracking Analysis (NTA), samples were prepared and split into two aliquots, one for analysis by each method. If samples were too concentrated for analysis by one method, they were diluted in the same manner as above, using nanopure water and 15 minutes bath sonication. Reported particle concentrations were corrected for the degree of dilution needed. Nanoparticle Tracking Analysis (NTA) was performed using a NanoSight LM10 instrument (NanoSight Ltd., Amesbury, United Kingdom), equipped with a 405 nm (blue) laser source, a temperature-controlled chamber, and a scientific CMOS camera (Hamamatsu). The sample (350–400 μL) was injected into the sample cell *via* a latex- and oil-free 1 mL syringe. A video (30 s) of each sample was collected and analyzed using NTA 2.3 Build 011 software (NanoSight Ltd.). The sample cell was then evacuated, rinsed and disassembled for further cleaning. All components were dried completely prior to reassembly. These

data collection and cleaning processes were repeated three times for each sample type. Results for number concentration (particles per mL) were averaged over the three replicates.

### Nanocomposite preparation for CNT release study

To prepare CNT/polymer nanocomposites a 20 mg mL<sup>-1</sup> aqueous stock solution of chitosan (Sigma-Aldrich,  $M_w = 20\ 000$ ) in 2 v/v% acetic acid (Fisher) was stirred and heated at 50 °C for approximately four hours. The stock solution was centrifuged with a Unico Powerspin LX at 4000 rpm to remove any undissolved solids. Carbon Solutions single-walled CNTs, known to contain trace yttrium catalyst, were then weighed into separate flasks and mixed in a 0.1, 0.5, 1, 2, 3, 4, and 5 wt/wt% with the chitosan stock solution to prepare well defined CNT–chitosan nanocomposites. Each suspension was stirred for approximately five minutes and sonicated for four hours with frequent stirring, creating a CNT suspension stabilized by chitosan macromolecules. After sonication, the suspension was centrifuged at 4000 rpm to remove any aggregates. 5 mL of each CNT–chitosan suspension and 5 mL of pure chitosan were then dried in aluminum dishes (44 mm diameter, 12.5 mm height, Fisherbrand) overnight; each composite was created from the same volume of the appropriate CNT/chitosan solution to ensure that they exhibited comparable size, shape and surface area. Once the coupons had dried, they were peeled from the aluminium dishes. The coupons were then soaked in a 1 M NaOH (Fisher) bath for 1 hour to remove excess acetic acid and washed with copious amounts of DI water.

Once prepared, the coupons were placed in 100 mL of DI water (see Fig. S1† for images) and left for 7 days. The CNT content of the nanocomposites varied from 0.1 wt% to 5 wt%, and included a control sample (0% CNT, *i.e.* pure chitosan). At the end of the 7 day period samples were collected from the surrounding DI water. Once collected, solid sodium deoxycholate was added to each aliquot to keep the CNTs dispersed prior to spICPMS analysis.

## Results

### CNT characteristics

To determine which metals should be investigated for possible detection by spICPMS, characterization of CNTs was performed by SEM-EDS. Although metal contents were provided by the manufacturers for each CNT, this analysis was carried out to verify manufacturers' claims and ensure there were no other metals which may be usable for spICPMS detection. Characterization data for size and metals content is given in Table 1.

Preliminary measurements using residual metals as a proxy for CNTs were done by monitoring multiple isotopes for each CNT studied, in order to ascertain the most effective analyte for each material. All metals which were identified in a particular CNT (see Table 1) were examined by spICPMS. Based on these preliminary results, the most readily observed metal isotope was used for the remaining analyses. This was done to avoid switching isotopes during spICPMS analysis.



**Table 1** Size characterization and percent metal for all CNTs used. Type of CNTs: SWNT = single-walled nanotube

CNT brand	Type	Length (nm)	Diameter (nm)	Metal content (manufacturer)	Metal content by EDS
Nanostructured and Amorphous Materials (NanoAmor)	SWNT	5000–15 000	1.1	Co 0.6%, Mo 0.1%, Mg 1.2% (at.%)	Co 0.5%, Mo 0.1%, Fe 0.1% (at%)
Carbon Solutions	SWNT	1800 ± 1000	3.8 ± 1.8	Ni, Y (1–30 wt%)	Ni 19.4%, Y 6.0% (at%)
Southwest Nanotechnologies	SWNT	578 ± 358	0.8 ± 0.1	Co, Mo (1–15 wt%)	Co 1.1%, Mo 3.7% (at%)

### Choice of element proxy

Metal content (Table 1) is an important consideration in choosing the analyte isotope, although there are other relevant factors. Choice of an analyte will be influenced by its isotopic abundance, and the potential for isobaric or polyatomic interferences on the isotopes. For example, although Ni is more abundant than Y in Carbon Solutions CNTs (19.6 wt% Ni *vs.* 6.0 wt% Y) by EDS analysis, the most abundant Ni isotope,  $^{58}\text{Ni}$ , is essentially unusable for ICP-MS analysis due to mass interferences with ArO, CaO, and Fe. As Y is monoisotopic at mass 89, it also gives a stronger signal than  $^{60}\text{Ni}$  (26.2% abundant) despite a greater relative amount of Ni in the CNT. For these reasons, Y was considered to be a more viable analyte (Fig. 1) for determining the presence of Carbon Solutions CNTs. Similar factors were considered in choosing  $^{59}\text{Co}$  as the analyte for NanoAmor and Southwest Nanotechnologies CNTs. Thus, although pulses were observed for all Mo isotopes analyzed, their abundances are distributed over seven isotopes, none being more than 25% abundant; the most viable Mo isotope,  $^{98}\text{Mo}$ , is 24.1% abundant. It has a higher background and fewer

large pulses are observed than for  $^{59}\text{Co}$ , which is also monoisotopic. For this reason  $^{59}\text{Co}$  was preferred as the metal isotope to analyze Southwest Nanotechnologies and NanoAmor CNTs (see Fig. 1).

Contributors to the background include instrumental (electronic) noise, isobaric interferences on the analyte isotope, and dissolved analyte. In the current application a low background is a crucial consideration as many CNTs will generate small pulses, due to either low metal content or small particle size, that are close to the background. This becomes clear when intensity data are binned, and the output is presented as a histogram of number of events (counts) on the y-axis *versus* the spICPMS response (signal intensity) on the x-axis as shown in Fig. S2.† This is a common approach used to interpret spICPMS data.<sup>25</sup> For each single walled CNT the metal analytes shown were chosen because of the low counts (<5 counts per dwell time) indicative of low instrumental noise and lack of interferences for that isotope. For example, the binned data for the Carbon Solutions SWNTs shows that the ICPMS response for  $^{89}\text{Y}$  as compared to  $^{60}\text{Ni}$  has a greater number of large pulses (ICPMS response >10) and a smaller number of “background” pulses (ICPMS response <5). Both factors favour using  $^{89}\text{Y}$  as compared to  $^{60}\text{Ni}$  for indirect SWNT detection.

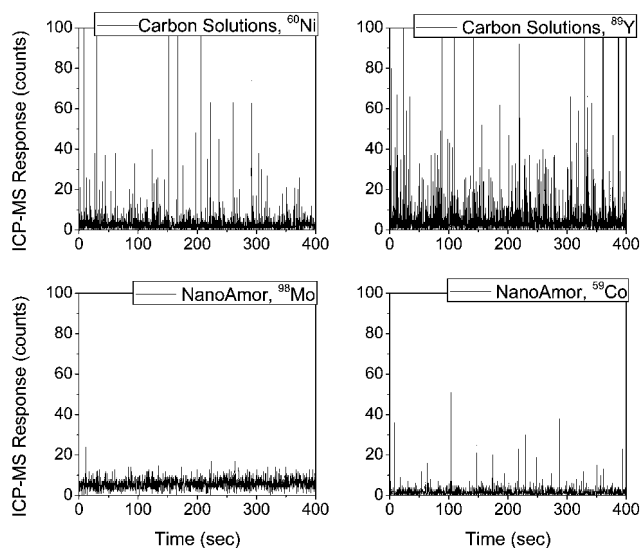


**Fig. 1** Real-time ICP-MS response data, for determination of the best analyte metal for CNTs used in this study. The CNTs were at  $1 \mu\text{g L}^{-1}$  to ensure enough CNTs would be in solution for analyte comparison. Only data for one isotope each of Ni ( $^{60}\text{Ni}$ ) and Mo ( $^{98}\text{Mo}$ ) are shown here. Other isotopes were not as usable due to mass interferences and lower isotopic abundances. For Carbon Solutions CNT,  $^{89}\text{Y}$  appears to have more pulses and more intense pulses above background, making it a better choice for detecting CNTs by this method. For NanoAmor and Southwest CNTs,  $^{59}\text{Co}$  is the clear choice over  $^{98}\text{Mo}$  for the same reasons.

### CNT pulse cut-off criteria

Once the most appropriate metal isotope had been identified for each CNT type it was important to determine the ICP-MS response for that particular analyte. This is necessary because the pulse intensity distribution from metals in CNTs can often run up against the background, making it difficult to discriminate signals from smaller masses of metal from the background. Conversely, the presence of dissolved ions can increase the background signal and cause underestimation of the particle number concentration, by masking the presence of small pulses arising from particles. We addressed this issue by determining if there was a difference in background counts between a DI blank and the supernatant of a CNT-containing solution. In these experiments, CNT samples were prepared and then centrifuged (1 hour, 125 000 Gs) to remove any CNTs. The supernatant was then diluted by factors equivalent to diluting the original CNT solutions to 200 and 400  $\text{ng L}^{-1}$ , so any dissolved metal ions which were released from the CNTs would be diluted by the same amount as that for CNT-containing solutions. Fig. 2 shows data where the DI blank and the 200  $\text{ng L}^{-1}$  equivalent dilutions of the supernatant are compared for each of the three CNT types (Nanostructured and Amorphous

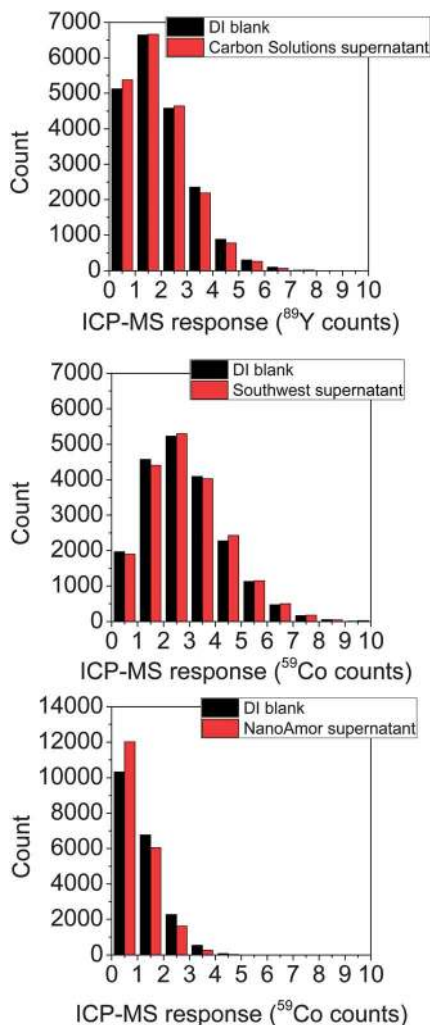


**Fig. 2** Comparison of the spICPMS response for DI blanks and CNT supernatant at the different metal isotope masses used for detection of each CNT. The ICP-MS response values for the DI blank and corresponding supernatant data for NanoAmor and Southwest Nanotechnologies SWCNTs, using  $^{59}\text{Co}$  as the analyte, are distributed differently because the analyses were performed on different days.

Materials, Carbon Solutions, and Southwest Nanotechnologies). The blank and supernatant means for  $^{89}\text{Y}$  had no significant difference ( $p < 0.05$ ) for Carbon Solutions CNT. Although there was a significant difference between the means for the Southwest Nanotechnologies and NanoAmor solutions ( $p > 0.05$ ), the upper tail of the signal distribution widths were similar enough that it can be assumed there is insufficient dissolved metal in CNT-containing solutions to affect discrimination of CNT pulses.

One of the main challenges in quantification of CNTs by spICPMS is the small fraction of metals in the materials. The low metal content means that there will be a less intense pulse for a given CNT than that for a material such as a gold nanoparticle, which is 100% Au on a per particle basis. This highlights the need to determine a pulse cut off criteria to discriminate pulses that correspond to CNTs from background signal. Fortunately, the similarity of the DI water and the supernatant spICPMS data for each of the three CNTs under

investigations demonstrates that a statistical analysis of DI blank data has the potential to provide the parameters needed to determine the most appropriate pulse cut-off criteria in CNT-containing solutions. Experimentally, we addressed the need for a quantitative approach in differentiating a pulse from background by comparing multiple analyses of a DI blank and a  $5 \text{ ng L}^{-1}$  concentration of Southwest Nanotechnologies CNTs. The goal was to determine if we could establish a protocol for establishing a standard cut-off above any instrumental or dissolved background for quantifying nanoparticulate pulses which would simultaneously minimize false positives in the blank and maximize pulses in the CNT sample. Both the DI water blank and the  $5 \text{ ng L}^{-1}$  CNT samples were run 30 times, for a total of 600 000 data points each, with the raw data shown in Fig. 3a and c. The reason for the low concentration was to have a small enough number of CNTs in solution, particularly ones that may appear near the background, that most of the ICP-MS counts would be equivalent to those in the DI blank. At a very low concentration, multiple runs (in this case 30) were performed to increase the volume of sample analyzed and allow for a larger number of CNT pulse events to be detected. The corresponding ICP-MS response distribution was binned up to 50 counts and is shown in Fig. 3b and d and to 10 counts in the inset figures to show the background ICP-MS response. Fig. 3 shows that differences between the DI blank and the CNT sample are only clearly seen above about 7–8 counts.

In Table 2 the mean ( $\bar{x} = 1.30$ ) and standard deviation ( $s = 1.17$ ) of the ICP-MS response were calculated by averaging all the data for the DI blank (Fig. 2(a)). Although it is clear that the background signals are not normally distributed (Fig. 2), we believe these statistical parameters provide the basis for differentiating small particle-created signals from the background noise. Indeed, this approach has been used by a number of researchers for studies of more uniform NPs.<sup>23,27</sup> Three different cut-off criteria for the ICP-MS response were examined to evaluate the number of false positives (apparent CNT detection events) in the blank and the ICP-MS response values (pulses) above the cut-off value which were considered to be CNTs.

Analysis of Table 2 reveals that with the lowest cut-off criterion ( $\bar{x} + 3s$ ), although the number of pulses counted as CNT detection events in the CNT solution was greatest (22 475), so was the number of false positives in the DI blank (7998, corresponding to 1.3% of the readings). The most conservative cut-off we tested was 10 counts, which was chosen after visual inspection of the data, and showed that in the DI blank nearly all of the ICP-MS response values were below this level. Table 2 shows that when using this more stringent cut-off criterion only 2 of 600 000 readings in the DI blank counted as pulses, but the number of pulses counted in the CNT solution was also reduced drastically, from the 22 475 observed with an  $\bar{x} + 3s$  cut-off criterion, to 81. The  $\bar{x} + 5s$  value (7.15) was deemed a good compromise between these cut-offs: 786 pulses were counted as CNT detection events in the CNT solution and only 84 in the DI blank. This corresponds to what is observed in the binned data (Fig. 3(b) and (d)), notably that the difference in the distributions between the DI blank and CNT solutions appears above 7 to 8 counts. Although in general we favor a statistical approach

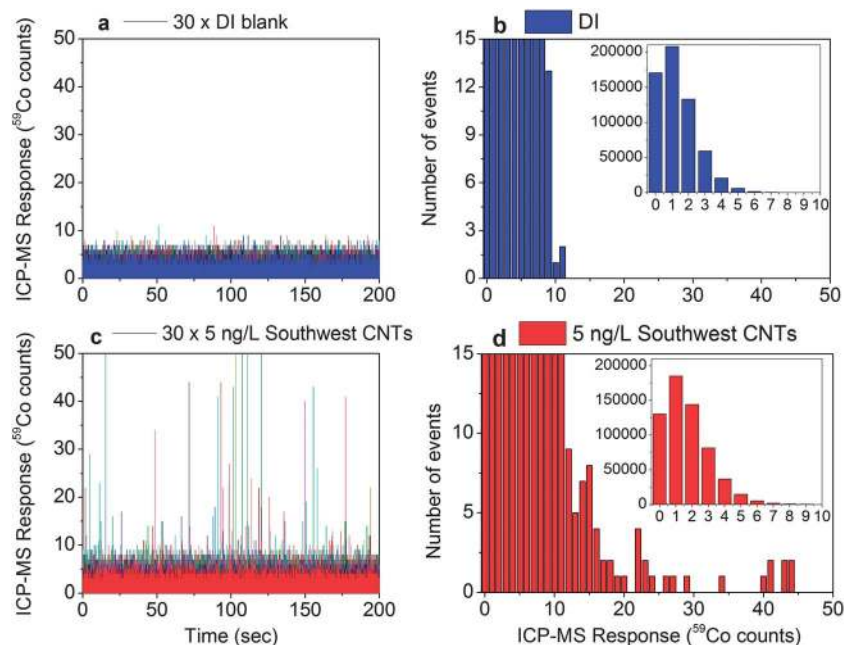


**Fig. 3** Comparison of DI blank and 5 ng L<sup>-1</sup> Southwest Nanotechnologies CNTs. Data show the sum of 30 individual runs corresponding to 600 000 readings. Panels (a) and (c) show real-time data for analyses of DI and 5 ng L<sup>-1</sup> CNTs, respectively, with (b) and (d) showing the ICP-MS response binned, illustrating where CNT pulses begin to become visible above the background. Insets in (b) and (d) show the similarity in the distribution of ICP-MS response for values  $\leq 7$  ("background").

**Table 2** Examination of different cut off criteria for differentiating CNT detection events from background signal. Values above each cut-off value were considered to be CNT detection events

Cut-off criterion	Calculated value from DI blank data ( $n = 600\ 000$ )	False positives in blank	Percent of total blank readings ( $n = 600\ 000$ )	Pulses above cut-off in 5 ng L <sup>-1</sup> Southwest Nanotechnologies CNT sample	Percent of total readings in 5 ng L <sup>-1</sup> Southwest Nanotechnologies CNT sample ( $n = 600\ 000$ )
$\bar{x} + 3s$	= 4.81	7998	1.3%	22 475	3.7%
$\bar{x} + 5s$	= 7.15	84	0.014%	786	0.13%
10	10	2	0.00033%	81	0.0135%

to defining the CNTs above background, we will demonstrate in the analysis of the CNT release studies that the choice of cut-off may be highly dependent on the experimental conditions.

### Quantification of CNT number concentration by spICPMS

Having established these analytical and data evaluation protocols, the ability of spICPMS to determine variable CNT concentrations was explored by analyzing a DI blank and solutions containing 200–800 ng L<sup>-1</sup> NanoAmor CNTs. To test the generality of this approach, we deliberately chose a different type of CNT from the Southwest Nanotechnology CNTs used to establish the cut-off criteria. To illustrate the effect that different cut-off criteria have on quantifying CNT concentrations, two values were used to discriminate nanoparticle pulses from the background signal as described in Table 2:  $\bar{x} + 3s$  and  $\bar{x} + 5s$  of the ICP-MS response values obtained from the DI blank. Analysis of Fig. 4 shows that in the CNT concentration range of 0–800 ng L<sup>-1</sup>, the number of pulses varies in proportion to the CNT concentration for both cut off criteria. However,

note the number of pulses detected in the DI blank for the  $\bar{x} + 3s$  cut-off criterion: 213 pulses out of 20 000 readings, for 1.07% of readings falsely identified as pulses. This is in line with the fraction of false positives reported in Table 2 for this criterion, and should be considered when selecting a cut-off. Although the increase in pulse number with increasing CNT concentration using this cut-off is clearly seen in Fig. 4, the afore-mentioned high background, and low linear correlation ( $r^2 = 0.732$ ) results in a weak proportional relationship. In contrast, the  $r^2$  value for the  $\bar{x} + 5s$  cut-off criterion ( $r^2 = 0.959$ ) is significantly improved, and more importantly shows more clearly that the number of pulses counted as CNT detection events is directly proportional to CNT concentration.

The number of CNT detection events can also be used to estimate the measured CNT concentration. The first step in calculating particle numbers is to determine the sample transport efficiency; the fraction of a given sample which reaches the plasma and is analyzed. This was accomplished following a method developed by Pace *et al.*<sup>25</sup> using a well-characterized, highly monodisperse Au nanoparticle (100 nm, BBI). Pulses

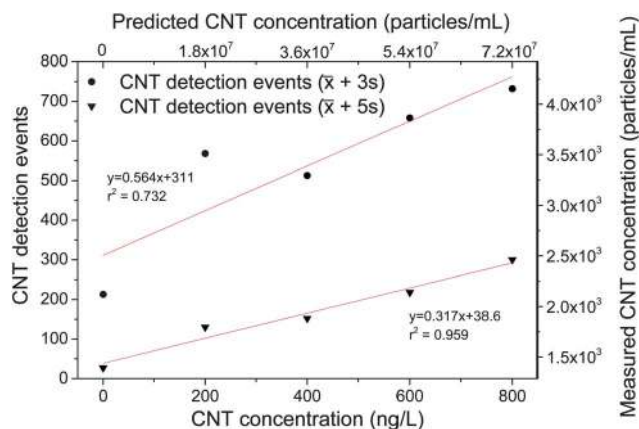


**Fig. 4** Relationship between CNT mass concentration ( $X$ ) and number of CNT detection events ( $Y$ ) for NanoAmor CNTs. Cut-offs of  $\bar{x} + 3s$  and  $\bar{x} + 5s$  based on the DI blank data were used to illustrate how different cut-off values affect the apparent number of CNT detection events. The number of pulses above the cut-off value was used to calculate a measured number concentration of CNTs in particles per mL using known flow rate, sample run time, and instrument transport efficiency. A predicted CNT number concentration for a given mass concentration is shown for comparison with the measured values, using data on the average CNT density, length, and diameter.

generated during spICPMS analysis of this Au NM can be related to mass of Au by a calibration curve generated by using dissolved Au, and mass is transformed to particle diameter based on the known density and volume of Au NMs. The calibration curve enables the transport efficiency term to be estimated. The transport efficiency term must be calculated for each day's analysis, as it has been observed to vary from day to day. For the data shown in Fig. 4 the measured transport efficiency was 0.050 (5.0% of sample volume reached the plasma) assuming that the transport efficiency of CNTs and Au NPs are comparable. For each mass concentration, the number of observed pulses was divided by the transport efficiency, flow rate ( $\text{mL min}^{-1}$ ), and sample run time (min) to obtain a value for measured particle number concentration (right Y-axis, Fig. 4).

To compare with the *measured* particle concentrations, the *predicted* CNT number concentrations for a given CNT mass concentration ( $\text{ng L}^{-1}$ ) can also be calculated using CNT length and width characterization data supplied by the manufacturer (Table 1). In the first step of this analysis the average volume of a single CNT was determined by multiplying the average length by the cross-sectional area, assuming a cylindrical geometry. This average volume was multiplied by the density ( $1.14 \text{ g mL}^{-1}$ ) to obtain the average mass of a single CNT. Finally, to determine the particle concentration (particles per mL) the mass concentration of a CNT solution ( $\text{mg mL}^{-1}$ ) was divided by the average mass of a single CNT ( $\text{mg per particle}$ ). It should be noted that uncertainties in the polydispersity in the dimensions (widths and lengths) of the CNTs and their degree of dispersion into individual tubes make this a gross approximation at best. Results from this analysis are shown in the top X-axis in Fig. 4.

A comparison of the measured and predicted CNT concentrations (Fig. 4) reveals that the concentrations measured by spICPMS were consistently about four orders of magnitude less than those predicted. As mentioned previously this is most

likely due to the significant variations in CNT metal content within CNT samples, with many CNT particles containing metal masses below instrument detection limit. Also, the CNTs may be present as bundles of tens to hundreds of particles, although the use of a surfactant to prepare the CNTs in solution was designed in part to maximize the number of individual CNTs present. In the spICPMS analysis, each bundle would only be counted as one pulse, resulting in severe undercounting of actual CNT concentrations.

### Comparison of spICPMS and NTA for CNT quantification

To further examine the discrepancy between measured and computed particle number concentration, Nanoparticle Tracking Analysis (NTA) was performed to directly measure CNT number concentrations. Solutions of three CNTs from NanoAmor, Southwest Nanotechnologies and Carbon Solutions were prepared at concentrations of  $10^{10}$  particles per mL calculated from size characterization data as previously described. These three samples were split for analysis by both NTA and spICPMS. The results for the comparison are shown in Fig. 5. The cut-off criterion for spICPMS analysis used for this experiment was  $\bar{x} + 5s$  of DI blank data.

The calculated particle number for a solution containing a known mass concentration of Au NMs matched well with both spICPMS and NTA measurements, providing confidence that both techniques can be accurate for quantification of a solution containing monodispersed spherical particles. However, the accuracy decreased for the moderately polydisperse, irregularly spheroidal,  $\text{TiO}_2$  (Sigma-Aldrich, measured size range  $\sim 40$  to  $400 \text{ nm}$ ), with values calculated from both NTA and spICPMS falling short of the calculated particle number. Consistent with

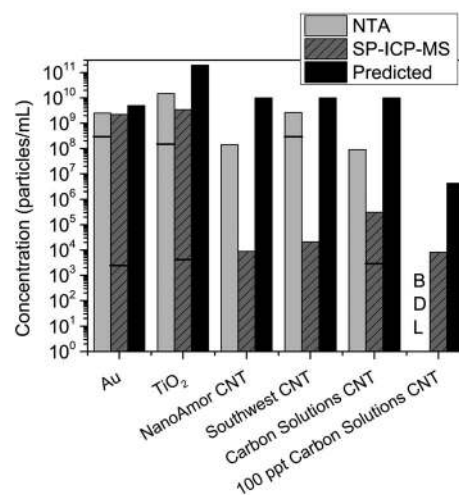


**Fig. 5** Particle number concentrations as measured by NTA and spICPMS for three types of CNTs. In addition to the CNTs, comparisons between the techniques were made using a highly monodisperse Au NM solution and a moderately polydisperse  $\text{TiO}_2$  NM solution. Horizontal black bars in columns indicate the diluted concentrations at which the measurements were made; these were then multiplied by the dilution factor to obtain the measured concentration of the undiluted solution. BDL – below detection limit.



the analysis presented in Fig. 4, the measured CNT particle number concentrations determined by spICPMS in Fig. 5 were  $10^3$ – $10^4$  particles per mL lower than those predicted based on the assumed average physical characteristics and at least  $10^2$  lower than those values measured by NTA. As mentioned previously, the likely reasons for this discrepancy are variations in metal content in individual CNTs, CNT bundling, as well as polydispersity in the CNT size/mass due primarily to length distributions. As shown by Jurkschat *et al.*,<sup>19</sup> the size of metal catalyst nanoparticles used in CNT synthesis can vary widely with smaller metal particles,  $\sim 5$  nm, intercalated non-uniformly in the CNT structure. We believe that the reason for the poor analytical sensitivity is because we are only observing CNTs which contain enough total metal mass to generate pulses above our chosen cut-off. This would correspond only to CNTs (or CNT bundles) which are large enough and contain a large number of metal nanoparticles and/or those which contain larger sized catalytic metal nanoparticles. In this respect, variations in the number and size of catalyst nanoparticles contained within individual CNTs will greatly affect the pulse height observed by spICPMS analysis, as the pulse height will be directly proportional to total mass of metal in a CNT. The variation in CNT size is also a factor; a smaller CNT containing the same percent metal as a larger CNT may not contain enough metal mass to generate a pulse which can be detected above the instrumental detection limit for that element.

Despite the undercounting of measured CNT number concentration, it is important to note that spICPMS exhibits superior particle number detection limit compared to other analytical techniques. For example, in the case of a  $100 \text{ ng L}^{-1}$  CNT solution made using Carbon Solutions CNT, the particle number measured by spICPMS is  $\sim 10^3$  particles per mL lower than that predicted from size data. However, at this low concentration thought to be representative of potential environmental releases, spICPMS was able to detect CNTs, while NTA results registered below detection limit (BDL).

### Detection of CNTs released from a polymer matrix

The incorporation of CNTs into polymer matrices to create a nanocomposite has been explored for a variety of materials, typically done to improve mechanical strength or conductivity of the material.<sup>28–30</sup> Release of CNTs from nanocomposites due to polymer degradation is a possible route of entry into the environment.<sup>31</sup> To probe the ability of spICPMS to detect CNTs released from these nanocomposites well-defined CNT composites were created by combining a known mass of CNTs (Carbon Solutions) and chitosan and placed in DI water. The extent of CNT release was studied for nanocomposites with varying mass percent CNT (sampled at 7 days) by analyzing an aliquot of the surrounding DI water by spICPMS. In collecting spICPMS data it is necessary to strike a balance between low particle number concentration and sufficient analysis time to allow a statistically relevant amount of data to be collected, as was demonstrated for polydisperse metal oxide nanoparticles and Ag nanowires.<sup>32</sup> Furthermore it has been shown that the total number of readings containing a particle should be less

than 5–15% to avoid coincidence events, where multiple particles enter the plasma simultaneously and are detected as a single pulse.<sup>26,27</sup> Initial analysis of the release samples indicated that a 1 : 200 dilution in nanopure water would be ideal to maximize the number of CNT detection events while minimizing coincidence. Longer analysis times were also used to increase the number of CNTs detected, in order to improve confidence in any observed trends. Thus, 100 000 readings were taken instead of the 20 000 used in the CNT characterization studies. This increased the analysis time of a single sample from 3.4 minutes to 17 minutes.

Fig. 6 shows the data acquired from spICPMS analysis of supernatant that contained different CNT loadings (0–5% by weight) in CNT–chitosan composites. Based on the previously discussed statistical analysis of spICPMS blanks, applying the  $\bar{x} + 5s$  criterion to the chitosan control sample (0% CNT) suggests a cut off of 1.37 counts. This value was the result of a low background obtained from the control sample (pure chitosan, 0% CNTs), with most readings being 0 or 1 count per dwell time. Thus, any data points at 2 or more counts would be considered a CNT-generated pulse using this criterion. After evaluating the number of data points that were at or above 2 counts for each sample, it became clear that this cut-off is not appropriate for examining the effect of loading on CNT release to solution (Fig. 6). This is particularly apparent in Fig. 6(c), where a cut-off value of 1.37 would require us to conclude that every sampling event corresponds to a CNT detection event due to the elevated background level. Given that the previous analysis of Carbon Solutions CNT supernatants suggest no release of dissolved yttrium, the elevated backgrounds for the higher loading, especially the 5% sample, implies a dramatic, non-linear increase in the number of low-metal content CNTs, which is physically unreasonable. However, it is also clear from a visual inspection of the raw ICPMS data that the number of

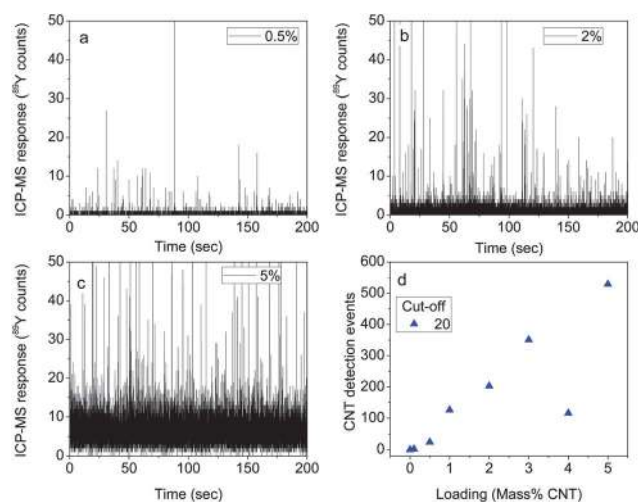


**Fig. 6** Examination of the effect of loading on CNT release from CNT–chitosan nanocomposites. Five samples were run for each analysis for a total of 100 000 readings. Real-time data for three individual CNT loadings of 0.5%, 2%, and 5% by mass are shown along with a plot of CNT detection events using a 20 count cut-off criterion.

CNTs released into solution does scale with the CNT loading in the polymer sample (compare Fig. 6(a)–(c)). Thus, it is apparent that the cut of criteria established in simple solutions (Fig. 4 and Table 2) are no longer valid in more complex aqueous conditions. Indeed, establishing appropriate cut-off criteria remains as a challenge which must be overcome if spICPMS is to be able to provide quantitative data on CNT concentrations in realistic environmental matrices. One possible solution to the background issue would be to determine a background cut-off criterion for each individual sample by comparing the ICPMS response function before and after the sample was ultracentrifuged to remove all of the CNT particles. By this approach sample-to-sample variations in the background signal could potentially be accounted for.

Accepting that the choice of an appropriate cut-off criteria is somewhat arbitrary at the present time and represents an area for future research and refinement, a visual inspection of the data with the highest background (5% loading) informed the choice of a 20 count cut-off where clearly all data above this point was due to detection of a CNT (Fig. 6(c)). Using this cut-off criterion, Fig. 6(d) shows that there is a linear correlation between the number of CNT detection events and the CNT loading. This relationship is qualitatively consistent with the changes observed in the ICPMS data shown in Fig. 6(a)–(c). We believe that these release studies provide a reasonable reflection of the current strengths and limitations of spICPMS in analysing CNTs in environmentally relevant scenarios. In terms of strengths, spICPMS offers significant advantages over other techniques in terms of particle number detection limits, and can also provide qualitative insights into how external variables (e.g. CNT loading in a polymer composite) impact the number of CNTs released. However, the changes in background shown in Fig. 6 also underscore the challenges of using spICPMS to provide unambiguous quantitative information on the concentration of polydisperse materials in all but the simplest of solutions (e.g. situation represented in Fig. 4), with CNTs representing an extreme example.

## Conclusions

Detection of CNTs using residual catalyst metals was found to be possible using spICPMS. The most effective metal for analysis depends on its chemical identity, abundance in the CNT as well as its natural isotopic abundance, and needs to be determined for each CNT. Although spICPMS was unable to quantify CNTs at concentrations used for NTA, it has the ability to detect the presence of CNTs at  $\text{ng L}^{-1}$  levels as well as to monitor increasing CNT concentration by detecting increasing pulse number. No other technique currently has this capability at such low concentrations. In simple solutions and with appropriate cut-off criteria the number of CNT detection events was found to be directly proportional to the number of CNT particles in the  $\text{ng L}^{-1}$  concentration range. In a more environmentally relevant application, spICPMS was shown to be able to detect and qualitatively determine relative changes in the concentration of CNTs released from a nanocomposite material. We believe that the current shortcoming of this technique

regarding quantification is rooted in the difficulties in establishing threshold values that can be applied in different situations and the inability of spICPMS to detect most of the comparatively small masses of metal incorporated within individual CNTs. The ability of spICPMS to differentiate a CNT pulse from background, however, could be improved with a greater efficiency of ion transport in the instrument quadrupole and a more sensitive mass detector. Even with the current situation which can best be described as a semi-quantitative ability to detect CNTs by metal proxy, there are potential applications. As environmental CNT concentrations have been predicted to be in the  $\text{ng L}^{-1}$  range, tracking of CNTs by this method would likely be possible in environmental and biological systems where the surrounding matrix would not be expected to contain pulses of metals such as Co, Y, Mo, or Ni. With our current ability to detect CNTs by spICPMS, we have demonstrated excellent concentration detection limit and ability to monitor relative increases in concentration, but are limited in accurate quantification of CNTs. Further development of this method for CNT analysis will focus on improving the accuracy of quantification.

## Acknowledgements

This work was supported by the NIH Grand Opportunities (RC2) program through NANO-GO NIEHS grant DE-FG02-08ER64613. D.H.F. would like to acknowledge partial financial support from the National Science Foundation (CHE-1112335).

## References

- 1 P. o. E. Nanotechnologies, Project on Emerging Nanotechnologies, <http://www.nanotechproject.org/inventories/consumer/>, accessed February 2012.
- 2 A. D. Maynard, P. A. Baron, M. Foley, A. A. Shvedova, E. R. Kisin and V. Castranova, *J. Toxicol. Environ. Health, Part A*, 2004, **67**, 87–107.
- 3 A. R. Murray, E. Kisin, S. S. Leonard, S. H. Young, C. Kommineni, V. E. Kagan, V. Castranova and A. A. Shvedova, *Toxicology*, 2009, **257**, 161–171.
- 4 K. Donaldson, F. A. Murphy, R. Duffin and C. A. Poland, *Part. Fibre Toxicol.*, 2010, **7**, 5.
- 5 C. A. Poland, R. Duffin, I. Kinloch, A. Maynard, W. A. H. Wallace, A. Seaton, V. Stone, S. Brown, W. MacNee and K. Donaldson, *Nat. Nanotechnol.*, 2008, **3**, 423–428.
- 6 F. Gottschalk, T. Sonderer, R. W. Scholz and B. Nowack, *Environ. Sci. Technol.*, 2009, **43**, 9216–9222.
- 7 B. Nowack, J. F. Ranville, S. Diamond, J. A. Gallego-Urrea, C. Metcalfe, J. Rose, N. Horne, A. A. Koelmans and S. J. Klaine, *Environ. Toxicol. Chem.*, 2012, **31**, 50–59.
- 8 N. C. Mueller and B. Nowack, *Environ. Sci. Technol.*, 2008, **42**, 4447–4453.
- 9 S. Kang, M. Pinault, L. D. Pfefferle and M. Elimelech, *Langmuir*, 2007, **23**, 8670–8673.
- 10 P. L. Ferguson, G. T. Chandler, R. C. Templeton, A. DeMarco, W. A. Scrivens and B. A. Englehart, *Environ. Sci. Technol.*, 2008, **42**, 3879–3885.

- 11 R. C. Templeton, P. L. Ferguson, K. M. Washburn, W. A. Scrivens and G. T. Chandler, *Environ. Sci. Technol.*, 2006, **40**, 7387–7393.
- 12 T. Belin and F. Epron, *Mater. Sci. Eng., B*, 2005, **119**, 105–118.
- 13 F. von der Kammer, P. L. Ferguson, P. A. Holden, A. Masion, K. R. Rogers, S. J. Klaine, A. A. Koelmans, N. Horne and J. M. Unrine, *Environ. Toxicol. Chem.*, 2012, **31**, 32–49.
- 14 D. S. Bethune, C. H. Kiang, M. S. Devries, G. Gorman, R. Savoy, J. Vazquez and R. Beyers, *Nature*, 1993, **363**, 605–607.
- 15 L. Ni, K. Kuroda, L. P. Zhou, K. Ohta, K. Matsuishi and J. Nakamura, *Carbon*, 2009, **47**, 3054–3062.
- 16 I. W. Chiang, B. E. Brinson, A. Y. Huang, P. A. Willis, M. J. Bronikowski, J. L. Margrave, R. E. Smalley and R. H. Hauge, *J. Phys. Chem. B*, 2001, **105**, 8297–8301.
- 17 X. Liu, L. Guo, D. Morris, A. B. Kane and R. H. Hurt, *Carbon*, 2008, **46**, 489–500.
- 18 X. Y. Liu, V. Gurel, D. Morris, D. W. Murray, A. Zhitkovich, A. B. Kane and R. H. Hurt, *Adv. Mater.*, 2007, **19**, 2790.
- 19 K. Jurkschat, X. Ji, A. Crossley, R. G. Compton and C. E. Banks, *Analyst*, 2007, **132**, 21–23.
- 20 C. Ge, F. Lao, W. Li, Y. Li, C. Chen, Y. Qiu, X. Mao, B. Li, Z. Chai and Y. Zhao, *Anal. Chem.*, 2008, **80**, 9426–9434.
- 21 K. X. Yang, M. E. Kitto, J. P. Orsini, K. Swami and S. E. Beach, *J. Anal. At. Spectrom.*, 2010, **25**, 1290–1297.
- 22 C. Degueldre and P. Y. Favarger, *Colloids Surf., A*, 2003, **217**, 137–142.
- 23 F. Laborda, J. Jimenez-Lamana, E. Bolea and J. R. Castillo, *J. Anal. At. Spectrom.*, 2011, **26**, 1362–1371.
- 24 D. M. Mitrano, E. K. Leshner, A. Bednar, J. Monserud, C. P. Higgins and J. F. Ranville, *Environ. Toxicol. Chem.*, 2012, **31**, 115–121.
- 25 H. E. Pace, N. J. Rogers, C. Jarolimek, V. A. Coleman, C. P. Higgins and J. F. Ranville, *Anal. Chem.*, 2011, **83**, 9361–9369.
- 26 R. B. Reed, C. P. Higgins, P. Westerhoff, S. Tadjiki and J. F. Ranville, *J. Anal. At. Spectrom.*, 2012, **27**, 1093–1100.
- 27 D. M. Mitrano, A. Barber, A. Bednar, P. Westerhoff, C. P. Higgins and J. F. Ranville, *J. Anal. At. Spectrom.*, 2012, **27**, 1131–1142.
- 28 V. H. Antolin-Ceron, S. Gomez-Salazar, V. Soto, M. Avalos-Borja and S. M. Nuno-Donlucas, *J. Appl. Polym. Sci.*, 2008, **108**, 1462–1472.
- 29 J. C. Grunlan, C. Yu, Y. S. Kim, D. Kim and K. Choi, *Abstr. Pap. Am. Chem. Soc.*, 2010, 239.
- 30 M. Moniruzzaman and K. I. Winey, *Macromolecules*, 2006, **39**, 5194–5205.
- 31 A. R. Kohler, C. Som, A. Helland and F. Gottschalk, *J. Cleaner Prod.*, 2008, **16**, 927–937.
- 32 R. B. Reed, C. P. Higgins, P. Westerhoff, S. Tadjiki and J. F. Ranville, *J. Anal. At. Spectrom.*, 2012, **27**, 1093–1100.